

## Microstructure and Slip Character in Titanium Alloys

D. BANERJEE

Defence Metallurgical Research Laboratory, Hyderabad-500258

J. C. WILLIAMS

Carnegie-Mellon University, Pittsburgh, PA, USA

Received 30 January 1986

**Abstract.** Influence of microstructures in titanium alloys on the basic parameters of deformation behaviour such as slip character, slip length and slip intensity have been explored. Commercial titanium alloys contain the hexagonal close packed ( $\alpha$ ) and body centred cubic ( $\beta$ ) phases. Slip in these individual phases is shown to be dependent on the nature of alloying elements through their effect on phase stability as related to decomposition into ordered or  $\omega$  structures. When  $\alpha$  and  $\beta$  coexist, their relative crystallographic orientations, size, shape and volume fraction, control the nature of slip. For a given composition, structure may be manipulated through appropriate thermomechanical treatment to obtain the desired deformation behaviour and therefore fracture mode.

### 1 . Introduction

Titanium alloys can exhibit perhaps the widest range of microstructures for a given alloy composition if both thermal and thermomechanical processing are employed to manipulate the **microstructure**.<sup>1,6</sup> If a range of alloy composition is also considered, then the range of microstructures which can be created in **Ti** alloys becomes extremely broad. As a result, the variations *in* the properties of **Ti** alloys can be extreme and have been shown to depend on microstructure to a significant extent. Because of the complexity of **Ti** microstructures', correlations between microstructure and properties have been difficult to develop and the current level of understanding of **structure-property** relations tends to rely more heavily on empirical correlations than on detailed mechanistic reasoning. However, in recent years the importance of fundamental

parameters such as deformation behaviour, e.g. slip character, slip length and slip intensity have begun to be recognized.<sup>6-11</sup> These parameters appear to play an **important** role in the strength, ductility, toughness and fatigue behaviour of a broad range of **alloys**.<sup>12-14</sup> It is possible, therefore, to gain considerable insight into structure-property relations by examining the influence of alloy composition and microstructure on deformation behaviour.

In this paper, existence of a wide range of slip character, slip intensity and slip length in **Ti** alloys have been shown. The factors which affect these parameters and describe the way in which microstructure and alloy composition affect them are discussed. The discussion is divided into three sections; the first deals with the deformation of the  $\alpha$  (hexagonal close packed) phase and the associated  $\alpha_2$  precipitate (based on the composition **Ti<sub>3</sub>Al**); the second examines the deformation of the  **$\beta$ -phase (body-centered cubic)** and the  **$\beta + \omega$ -phase** mixtures; the third describes slip processes in commercially important alloys containing  **$\alpha + \beta$ -phase** mixtures. Some correlations between slip character, length and intensity and properties have been described. Some ways in which the correlations can be used to tailor the properties of **Ti** alloys have been suggested.

## 2. Deformation of the $\alpha$ -Phase

The hexagonal  $\alpha$ -phase of **Ti** deforms both by slip and **twinning**.<sup>15</sup> Discussion in this section, have been restricted to slip character. Unalloyed  **$\alpha$ -Ti** can slip on basal, **prismatic**<sup>1</sup> and first and second order pyramidal planes and both  $\bar{a}$  as well as  $\bar{c} + \bar{a}$  slip have been **observed**.<sup>16-19</sup> These slip systems are summarized in Table 1. The commercially

Table 1. Deformation Modes in  $\alpha$ -Ti

Slip systems	$\{0001\}$	$\langle 11\bar{2}0 \rangle$	} $\bar{a}$ slip
	$\{10\bar{1}1\}$	$\langle 1\bar{1}20 \rangle$	
	$\{10\bar{1}2\}$	$\langle 11\bar{2}0 \rangle$	
	$\{1\bar{1}22\}$	$\langle 11\bar{2}3 \rangle$	} $\bar{c} + \bar{a}$ slip
	$\{10\bar{1}1\}$	$\langle 11\bar{2}3 \rangle$ I	
Twin systems	$\{10\bar{1}2\}$ , $\{11\bar{2}1\}$ , $\{11\bar{2}3\}$ ,	c-axis extension	
	$\{11\bar{2}2\}$ , $\{11\bar{2}4\}$ , $\{10\bar{1}1\}$	c-axis reduction	

important alloying elements which have any significant solubility in  **$\alpha$ -Ti** are Al and O. These also have a prominent effect on slip behaviour.<sup>6,11,6,20</sup> Oxygen is always present in  **$\alpha$ -Ti**, but at low concentrations ( $\leq 1500$ wt ppm) the slip is wavy, whereas at higher

concentrations it becomes planar. As the *Al* content of *Ti* is increased, the slip mode becomes increasingly planar and coarse. This change is particularly prominent between 2 and 4 wt per cent *Al* and is often attributed to an increase in short range order (SRO) of *Al* atoms in the  $\alpha$  lattice. At aluminium concentrations high enough to precipitate fine coherent particles of the ordered  $\alpha_2$ -phase (based on  $Ti_3Al$ ), planar slip becomes even more intense. These features are all illustrated in Fig. 1. This transition from homo-

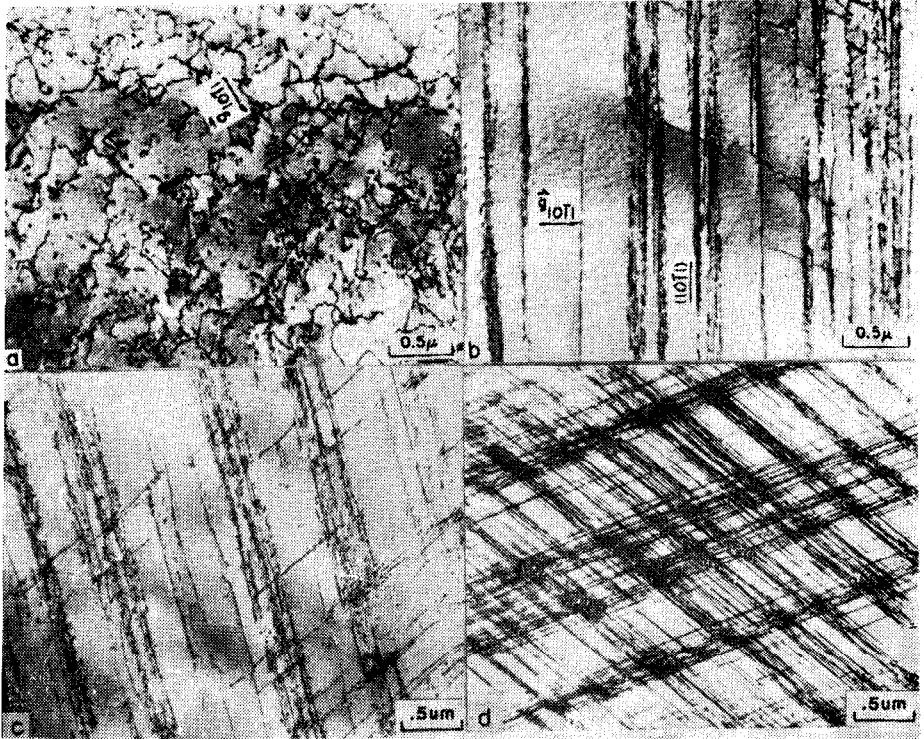


Figure 1. Deformation of the s-phase : (a) pure *Ti* with < 1000 ppm oxygen (b) *Ti*~5000 ppm  $O_2$  (c) *Ti*-4 wt per cent *Al* (d) *Ti*-6 wt per cent *Al*.

geneous slip to planar slip occurs as a result of localized strain softening on active slip planes. This is due to the passage of dislocations through regions of SRO, or coherent ordered particles (Fig. 2) which results in a disruption of these regions either by dissolution and shear of  $\alpha_2$  or local reductions in SRO. This mechanism for slip localization is distinct from any effect of alloying additions on stacking fault energy and reduced cross slip behaviour as observed in fcc metals and alloys. In fact, planar slip due to reductions in stacking fault energy is, in a sense, opposite to that due to SRO since in the former slip plane hardening occurs and in the latter softening occurs.

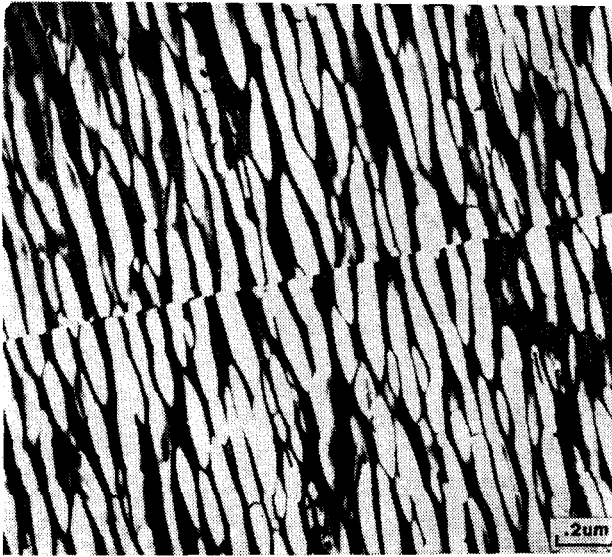


Figure 2. Shearing of the  $\alpha_2$ -phase by a slip band in a *Ti-Al* alloy. Dark field  $\alpha_2$ -phase.

Luetjering & Weissmann<sup>7</sup> have shown that slip localization in an alloy containing  $\alpha_2$  depends on the ability of the dislocations to shear the precipitates. If the precipitate size is increased and the volume fraction decreased so that the stress required to bypass the precipitates is lower than that to shear them, a more homogeneous dislocation distribution results.

It is important to note that  $\alpha_2$  precipitation promotes coarse planar slip on prismatic rather than pyramidal planes.<sup>7</sup> This effect is opposite to that of oxygen which promotes coarse planar glide on pyramidal planes. At sufficiently rich oxygen concentrations and low aging temperatures, ordering of oxygen in interstitial sites, according to Churchman,<sup>16</sup> leads to interference with slip on all basal and prismatic planes, but only half the pyramidal planes, thus decreasing the CRSS on this latter set of planes. It is important to remember that oxygen also increases the volume fraction of  $\alpha_2$  at a given aluminum content. Therefore, at aging temperatures high enough to form  $\alpha_2$  precipitates, this second effect of oxygen is also important.

### 3. Deformation of $\beta$ -Phase and $\beta$ -Phase Alloys

The  $\beta$ -phase in *Ti* alloys is BCC and, as such, might be expected to deform by pencil glide<sup>21</sup> as in the case of *Fe* and other BCC materials. In general, this is not the case. The  $\beta$ -phase can exhibit slip,<sup>22</sup> twinning<sup>23</sup> or stress assisted martensite<sup>7,24</sup> as the result of plastic deformation. The mechanical behaviour of the  $\beta$ -phase varies widely depending

on which of these deformation modes occurs. In this section, these variations are outlined and some reasons are suggested for such diverse behavior,

The most important variable which determines the deformation behaviour of  $\beta$ -Ti is alloy composition.<sup>22,23</sup> This composition sensitivity is manifested through the relation between composition and constitution, not through more intrinsic factors such as stacking fault energy as in the case of FCC alloys.<sup>25</sup> It is not intended to provide an exhaustive account of the decomposition of P-phase; rather, it is desired to outline the complexity of the situation because it is this that forms a basis for understanding the deformation behavior.  $\beta$ -Ti can decompose athermally to form the  $\omega$ -phase which exists as a high density of small, coherent precipitates. The temperature sensitivity of a thermal  $\omega$ -phase formation is strong, therefore small changes in deformation temperature can lead to large shifts in the constitution of the alloy.<sup>26</sup> With increasing concentration of p-stabilizing solutes the temperature at which the athermal  $\beta \rightarrow \omega$  transformation occurs decreases. Thus, increasing concentrations of Mo, V, Fe, Cr and other  $\beta$ -stabilizers lead to retained  $\beta$ -phase that does not contain the  $\omega$ -phase. Moreover, the  $\beta \rightarrow \omega$  transition is preceded by a complex lattice softening which leads to an extensive array of diffuse intensity in electron diffraction patterns.<sup>28</sup>

At low solute concentrations, just sufficient for retention of the  $\beta$ -phase without the formation of martensite, the P-phase deforms by slip, twinning or the formation of stress assisted martensite. Although these various deformation modes have been studied in detail, there is not a clear picture as to why they occur. At higher solute concentrations the  $\beta$ -phase deforms only by slip, but the slip is very planar and tends to be concentrated in localized bands," as shown in Fig. 3. The intensity of these bands decreases with increasing solute content but the bands tend to remain planar, especially for a BCC material. The reasons for this appear to be related to the

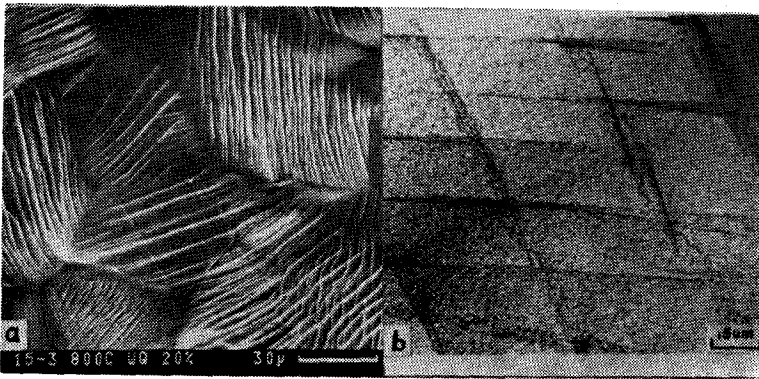


Figure 3. Slip behaviour of the B-phase in  $Ti-15-V-3Al-3Cr-3Sn$ : (a) surface slip after 20% elongation of tensile sample, and (b) TEM of slip bands on {110} planes.

presence of **pre- $\omega$**  transformation defects in the e-phase. These defects are also responsible for the diffuse streaking in electron diffraction patterns mentioned earlier. The detailed nature of these defects have been discussed **elsewhere**.<sup>26</sup> It is **sufficient** here to compare them to an atom position equivalent of short range order. That is, these defects represent localized regions where the lattice is distorted and the extent of this distortion is altered by moving dislocations so that subsequent dislocations experience a reduced flow stress. This leads to a localization of flow in a manner similar to that which occurs when short range order exists. Such localization also tends to exclude easy cross slip as is often observed in BCC metals.

If metastable  **$\beta$ -phase** alloys are aged to precipitate isothermal w-phase, the flow stress increases significantly<sup>13,27</sup> but the ductility is simultaneously reduced. This loss in ductility is associated with the formation of intense planar slip bands. These bands appear to form as a result of shearing of the coherent isothermal w-phase precipitates (Fig. 4). Further, specimens aged to a smaller w-phase volume fraction exhibit a reduction in work hardening rate which is consistent with shearing of coherent precipitates and strain localization. Fracture under these conditions is either intergranular, grain boundary cracking being initiated by pile-up stresses at the blocked slip bands, or it may occur along the slip bands themselves.<sup>12,13</sup> Which of these mode **soccur** depends on grain size and **the** intensity of Slip **localization**. In either case, fracture is microscopically ductile, that is, it occurs by microvoid coalescence, but the strain localization leads to a macroscopic embrittlement. It is interesting to note that if the  $\omega$  volume fraction is reduced to increase the interparticle spacing, dislocations may be induced to bypass the w **particles**.<sup>13</sup> However, here, as in the case of  $\alpha_2$  precipitation in the  $\gamma$ -**phase**,<sup>11</sup> the increments in strength obtained when a bypass mechanism is operative are no longer attractive.

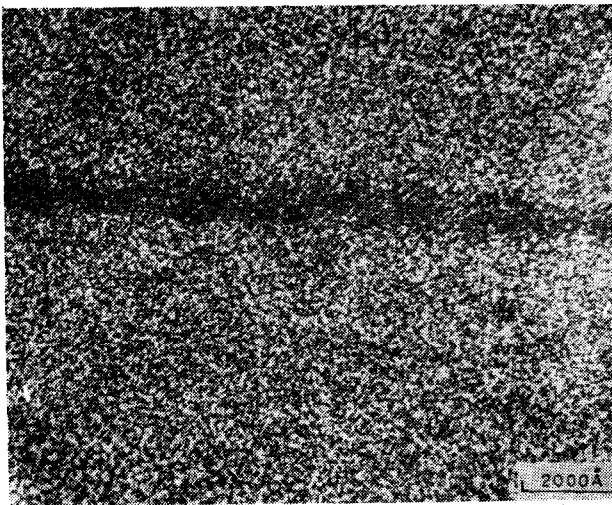


Figure 4. Shearing and dissolution of  $\omega$  particles within a slip band in a *Ti-Mo* alloy.

#### 4. Alloys Containing $\alpha$ and $\beta$ -Phases

Most commercial titanium alloy microstructures are based on mixtures of the  $\alpha$  and  $\beta$ -phases. The morphology and distribution of these phases can vary widely depending upon alloy composition and heat treatment.

As a preamble to this section, it is noted that the  $\beta \rightarrow \alpha$  transformation crystallography plays an important role in determining slip character in these alloys. The  $\alpha$ -phase forms from  $\beta$  as a plate or lath-shaped product according to the Burgers orientation relationship. This crystallography allows a close parallelism between four prominent slip systems in the  $\alpha$  and  $\beta$ -phase for a given variant of the  $\alpha$ -phase. For the particular variant  $(0001)_\alpha \parallel [011]_\beta; [2\bar{1}10]_\alpha \parallel [111]_\beta$ , these are

$$(011) [111]_\beta \parallel (0001) [\bar{2}110]_\alpha - \text{basal slip}$$

$$\left. \begin{array}{l} (110) [\bar{1}\bar{1}1]_\beta \parallel (01\bar{1}1) [2\bar{1}\bar{1}0]_\alpha \\ (\bar{1}01) [1\bar{1}1]_\beta \parallel (0\bar{1}11) [\bar{2}1\bar{1}0]_\alpha \end{array} \right\} - \text{pyramidal slip}$$

$$(\bar{2}\bar{1}1) [1\bar{1}1]_\beta \parallel (0\bar{1}10) [2\bar{1}\bar{1}0]_\alpha - \text{prismatic slip}$$

Thus, out of the many possible slip systems in the  $\alpha$  and  $\beta$ -phases, four permit easy transfer of slip from one phase to another. This process is complicated by the fact that the  $\alpha/\beta$  interfaces are generally semicoherent and contain periodic arrays of 'c' type dislocations and ledges. Thus, the glide dislocations involved in the process of slip transfer would be forced to interact with these interface dislocations. The products of these interactions are expected to be complex and some of them will not be glissile.

Thermomechanical processing below the  $\beta$ -transus can be used to alter the morphology of the  $\alpha$ -phases to a more equiaxed product. In consequence, the  $\alpha/\beta$  interfaces of such an equiaxed product would be substantially disordered in comparison to plate  $\alpha$ , and the Burgers crystallography is usually destroyed as well. Slip transfer across these equiaxed  $\alpha$  interfaces can therefore be expected to be a more difficult process.

#### 5. Near $\alpha$ Alloys : The $\beta$ Heat Treated Structure

In Alloys with a low concentration of  $\beta$  stabilizing additions (near  $\alpha$  alloys), the transformation from  $\beta$  to  $\alpha$  cannot be suppressed by quenching from the  $\beta$ -phase field. After such a quench, near- $\alpha$  alloys contain a structure characterized by the formation of lath or plate shaped  $\alpha$  in prior  $\beta$  grains whose size is determined by the heat treatment temperature in the  $\beta$ -phase region. The  $\beta$  volume fraction of these alloys is typically about 5 per cent. These alloys and this class of microstructures are used to attain high creep strength but often have comparatively low tensile ductility and fatigue life in this microstructural condition. An important heat treatment variable for this

class of microstructures is the cooling rate from the  $\beta$  region.<sup>25</sup> Figure 5 illustrates the manner in which microstructure varies with cooling rate. As the cooling rate decreases, laths become coarser and show an increasing tendency to form colonies of laths with the same orientation variants. The slower cooling rates are also accompanied by a decrease in the dislocation substructure within the  $\alpha$  laths as shown in Fig. 5. The deformation behaviour varies markedly with these changes in microstructure. The water-quenched martensitic samples can fail by intergranular fracture suggesting that most of the deformation has been concentrated in the small grain boundary  $\alpha$  allotriomorphs present in this microstructure." More slowly cooled samples exhibit

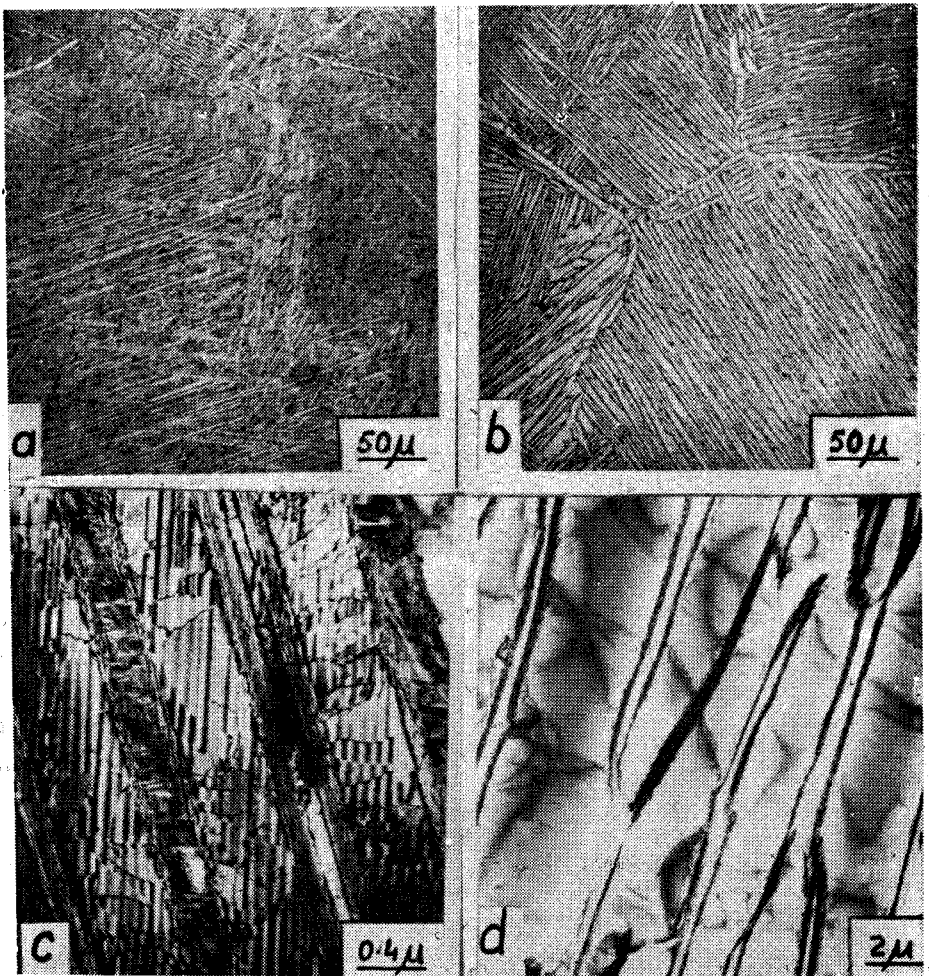


Figure 5. The effect of cooling rate from the B-phase region on the microstructure of  $Ti-6Al-3Mo-1.5Zr-0.25Si$ : (a) air cool (b) furnace cool, (c) stacking faults with the  $\alpha$ -phase in air-cooled sample, and (d) dislocation free  $\alpha$ -phase in furnace-cooled sample.

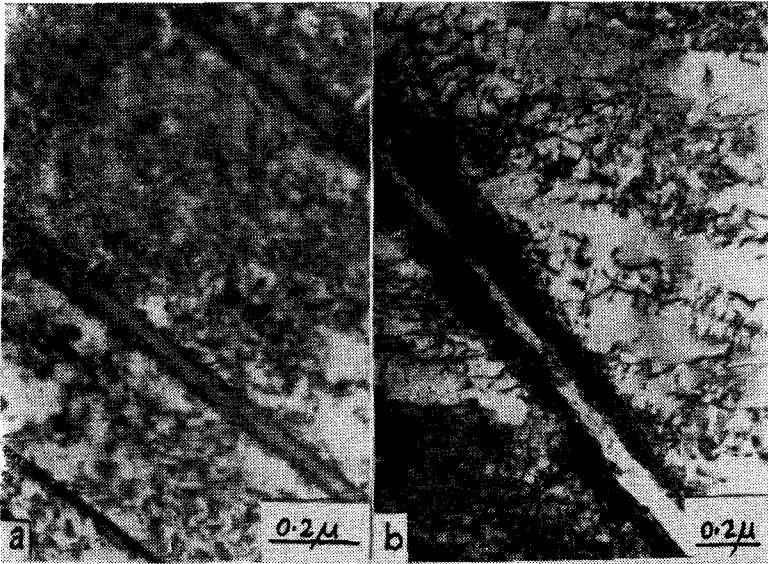


Figure 6. The variation of slip character with cooling rate from the P-phase region in  $Ti-6Al-3Mo-1.5Zr-0.25Si$ .

transgranular ductile fracture mode, slip becomes increasingly planar and localized with slower cooling rates as shown in Fig. 6.

This change in slip mode is viewed as being essentially related to the change in microstructure. A colony of similarly oriented  $\alpha$  variants can essentially be viewed as a single grain of the  $\alpha$ -phase, this being particularly so since, as discussed earlier, the Burgers relationship allows the existence of several common slip systems between the  $\alpha$  plates and the  $\beta$  layers retained between them. As the colony size increases, certain slip planes emerge as those on which the mean free path for slip extends from one end of the colony boundary to another. Note also that adjacent colonies can share a common basal plane for the  $\alpha$ -phase through the Burgers crystallography, further extending the slip length for this slip system. Glide dislocations, therefore, are preferentially concentrated on these slip systems. This effect is amplified by the decreasing substructure density within the  $\alpha$ -phase: Fig. 7, which shows slip bands extending across an entire colony, illustrates this point. Extremes of slip planarity and coarseness, which may be induced by  $\alpha_0$  formation or high oxygen levels, can lead to a localized transgranular fracture mode, with fracture occurring along slip bands (Fig. 8). Such fractures occur locally by a ductile fracture mechanism but at low macroscopic strains.

It is emphasized here that little or no work has been carried out to investigate the effect of the retained  $\beta$  layers on slip mode in these types of structure. The composition and hence the strength of  $\beta$ , its thickness and continuity, the presence or absence of  $\omega$

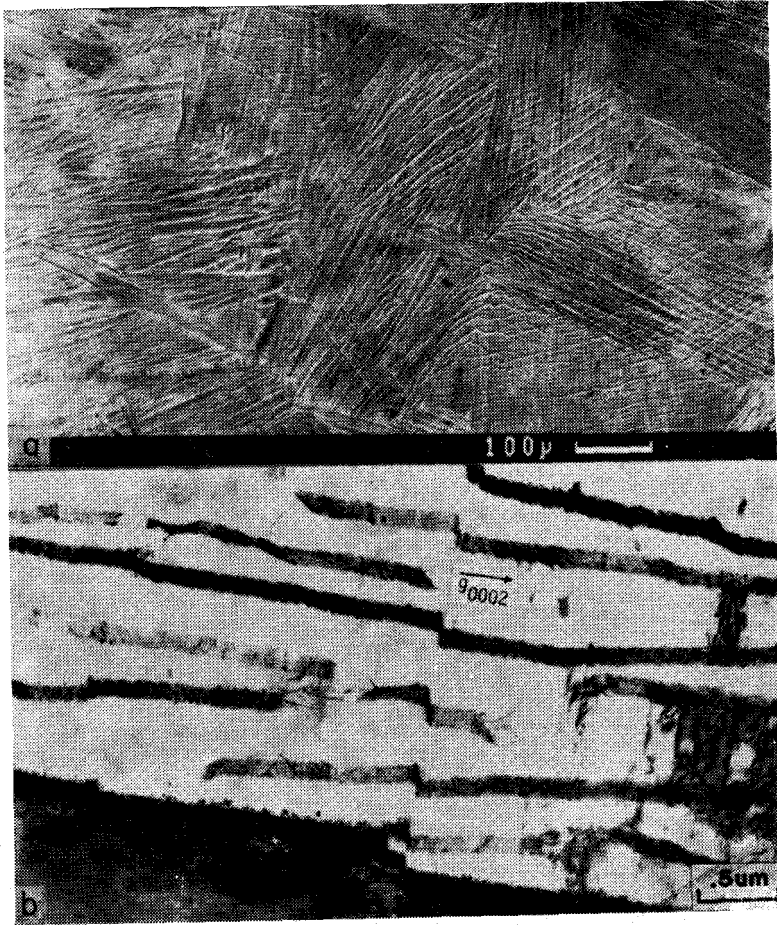


Figure 7. (a) Surface slip in a near-z *Ti* alloy. Slip bands extend across entire colonies, and (b) Shear of  $\alpha$  and  $\beta$  phases by basal slip within a colony.

within the  $\beta$  are all factors which would influence the ease of slip transfer across the  $\beta$  layers, and hence the development of planar slip.

## 6. Metastable $\beta$ Alloys

Alloying additives such as *V*, *Mo*, *Cr* and *Fe* allow the metastable retention of the  $\beta$ -phase at room temperature by shifting the TTT curves for a precipitation towards longer times and suppressing  $M_s$  below room temperature. The  $\beta$ -phase in such alloys may then be isothermally aged to form  $\alpha$ -phase precipitates whose size and distribution is substantially finer than that possible in the near-*u* alloys. Recent work<sup>29</sup> on the newly developed commercial titanium alloy *Ti-15V-3Cr-3Al-3Sn* illustrates some typical effects of a precipitation on slip character. This alloy is uniquely suited to this kind of study since it does not form continuous films of grain boundary  $\alpha$  on aging at temperatures below 600°C, nor does it form  $\omega$ -phase on low temperature aging, both factors

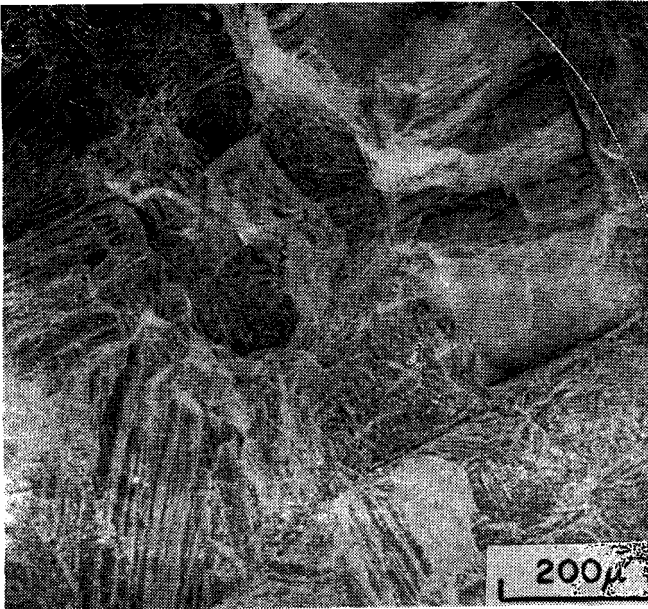


Figure 8. Fracture along slip bands in *Ti-6Al-3Mo-1.5Zr-0.25Si* associated with extreme slip localization.

which affect the deformation and fracture behaviour of this class of alloys. Fig. 9 illustrates the range of  $\alpha$  precipitate distributions developed on aging *Ti-15V-3Cr-3Al-3Sn* at various temperatures and the associated tensile strength and ductility for these.

Slip in the B-phase of this alloy is essentially planar and occurs primarily on (110) planes (Fig. 3). The alloy exhibits a low work hardening rate in the as-quenched state and failure occurs by necking after true strains of about 15%. The microstructure produced by low temperature aging (Fig. 9c) results in a complete loss of ductility and this embrittlement can be directly related to the slip behaviour which has become much coarser (Fig. 10). The exact mechanism by which this hyper-fine  $\alpha$  distribution concentrates deformation into narrow intense slip bands is not completely clear since the  $\alpha$  particles are neither ordered nor coherent with the matrix, the two major contributing factors towards slip localization in precipitation hardened systems.<sup>10-13</sup> It is also noted that this kind of slip localization is also observed in other *Ti* alloy systems where the  $\alpha$  morphology is different (though the particle sizes are as fine).<sup>30</sup> It appears then that when the  $\alpha$  particles are very fine and their volume fraction is very high, the only mode by which the material can deform is by particle shearing. This leads to the intense slip localization observed in Fig. 10. Aging at slightly higher temperature to increase  $\alpha$  precipitate size results in similar strength levels without the attendant loss in ductility. In this case, the slip distribution is much finer (Fig. 11). The finer slip distribution also is accompanied by an increase in the work hardening rate over that of the unaged  $\beta$  matrix. This behaviour is consistent with the discussion

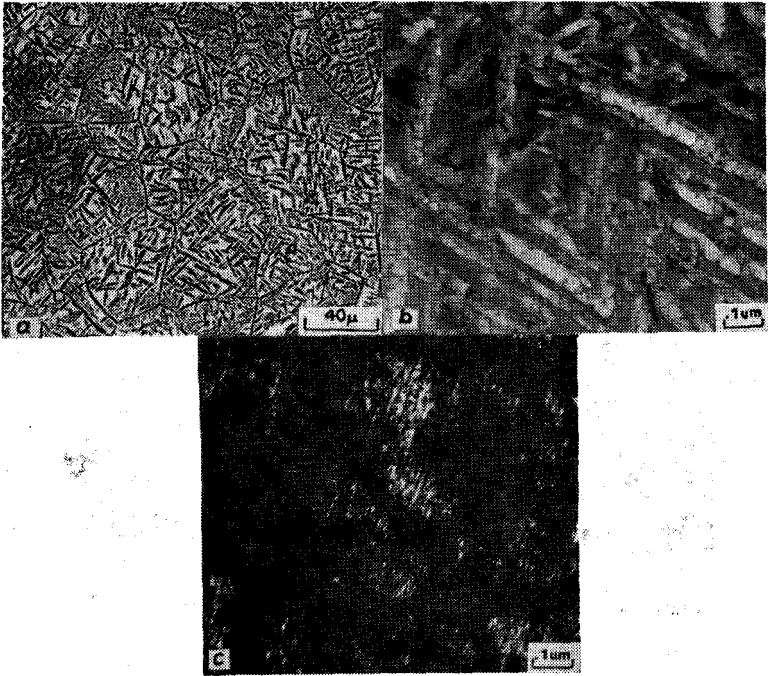


Figure 9.  $\alpha$  precipitates in a  $\beta$  matrix in *Ti-15V-3Al-3Cr-3Sn* : (a) aged at 600°C (*UTS* = 900MPa, *El.* = 20%), (b) aged at 450°C (*UTS* = 1400 MPa, *El.* = 8%), and (c) aged at 300°C (*UTS*=1400 MPa, *El.* = 0%).

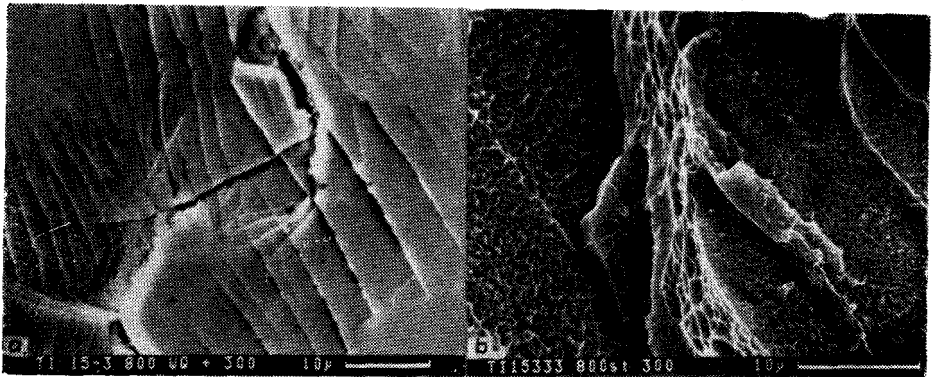


Figure 10. (a) Surface slip in a sample of *Ti-15V-3Al-3Cr-3Sn* aged at 300°C and deformed in tension. Note cracking along slip bands and at grain boundaries and compare with Figure 3 and, (b) associated fractograph shows faceted fracture with evidence of dimple formation on the facets.

of slip transfer presented in the initial portion of this chapter. That is, a single system in the  $\beta$ -phase matches with a slip system of the  $\alpha$ -phase in only 3 out of 12 possible

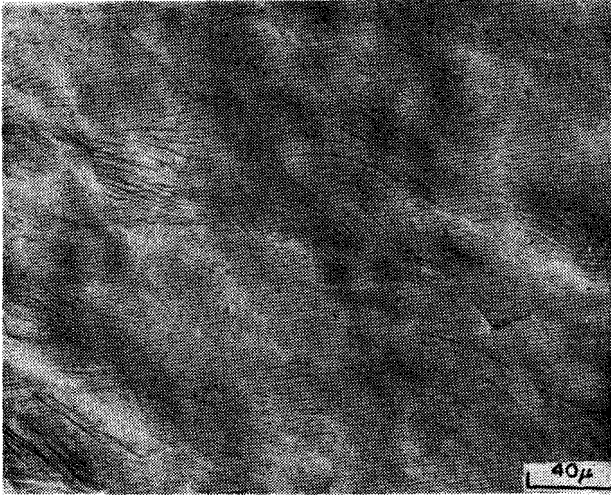


Figure 11. Slip distribution in *Ti-15V-3Al-3Cr-3Sn* aged at 450°C and deformed in tension.

a variants. Thus, in microstructures such as in Fig. 9 (a), (b), where different a variants are randomly distributed, the mean free path for slip on a single slip system is **confined** to the interparticle spacing of the a-phase. This situation is in contrast to the case of the colony type structures presented **previously**. Slip localization thus does not occur when the a lath size is sufficiently large.

#### 7. $\alpha + \beta$ Alloys with Equiaxed Primary a

Hamajima, Luetjering and **Weissmann**<sup>31</sup> made several unique observations on the effect of primary a size and distribution on deformation behaviour in a *Ti* alloy. **They** observed that small equiaxed primary  $\alpha$  particles work-harden more rapidly than the surrounding matrix, so that they become hard particles in a soft matrix after a certain amount of strain. If the interparticle spacing is then small enough for an 'interaction' to exist between these 'hard' particles, slip tends to localize between **them**<sup>31</sup> leading to losses in ductility. If, however, the primary a particles are relatively larger, then matrix and the  $\alpha$  particles work-harden similarly and this effect is not observed. Similar effects have been observed recently in a *Ti-10V-2Fe-3Al* alloy.<sup>24</sup>

#### 8, Implications Regarding Properties

Slip mode has an important effect on the properties of *Ti* alloys. For example, it has been known for some time that *Al* concentrations in excess of  $\sim 8.5$  wt % caused embrittlement of the  $\alpha$ -phase<sup>32</sup>. Later it was shown that this composition permitted the

**formation** of significant volume fractions of the  $\alpha_2$ -phase.<sup>33</sup> Only recently has the effect of  $\lambda_2$  on slip mode and the relationship between strain localization and low ductility been **recognised**.<sup>8</sup> A similar historical picture could be **developed for  $\omega$ -phase embrittlement** of  $\beta$ -phase. Here also the formation of large volume fraction of a coherent precipitate leads to strain localization and dramatic reductions in ductility. **It** is intriguing to contrast these two cases, however. In the case of  $\alpha_1$  u-phase embrittlement, there **also** is a fracture mode transition to a cleavage **fracture**,<sup>8</sup> whereas in the  $\omega$ -phase embrittlement case the low ductility fracture is accompanied by large local strain as mentioned earlier. Several models<sup>34-36</sup> have been suggested to account for the onset of cleavage fracture, but none of these seem to adequately explain all of the available data. The point we wish to make here is that an understanding of the effect of slip mode on ductility has been helpful in explaining composition and heat treatment effects but that this viewpoint is not a panacea which permits all variations in mechanical behaviour to be explained in a truly fundamental way. Slip character can affect the fracture behaviour differently depending on whether general yielding or local **yielding is involved**.<sup>37</sup> Thus, tensile ductility and fracture toughness may be affected differently by variations in slip character. That is, in the case of local yielding, strain localization can lead to crack branching and deviation which can actually increase the energy required to extend the crack and increase the toughness. Thus, in the case of fracture toughness, the relative contributions of variations in fracture path and **local** crack extension energy determine the net effect of variations in slip mode on toughness. In the case of general yielding, strain localization also reduces the work hardening rate and this can enhance crack initiation and lower the crack **extension** energy with a reduction of **ductility**.

The effect of slip mode on fatigue properties also is substantial and, as in the case of fracture, depends on which aspect of fatigue is under consideration. Strain localization reduces the resistance of a material to fatigue crack initiation but can enhance the fatigue crack propagation characteristics. Thus, for applications that are limited by crack initiation, care should be exercised to avoid material compositions or heat treatment conditions that promote strain localization. For crack growth limited applications, on the other hand, improvements in performance can be realized if materials which exhibit strain localization are used.<sup>3,5,26</sup> Further, coarse **grained** materials which exhibit strain localization tend to have better fatigue crack growth resistance than do the same ones with fine **grains**.<sup>3,5,26</sup> While such changes in material characteristics improve the fatigue crack growth performance, the same changes can have such adverse effects on ductility, strength and fatigue crack initiation resistance that they cannot be tolerated. **It** is indeed rare for an application to be so completely dominated by a **single property** requirement that this property can be optimized at the significant **expense** of other properties.

**In** summary, **slip** mode has an important effect on the fracture-related properties of high strength alloys. **In** some cases it is possible to select heat treatments that affect the slip mode in a way which improves a particular property. In general, an

understanding of the relationship between slip mode and properties permits the behaviour of a given material or material condition to be explained. Thus, the emerging importance of slip character in providing an improved understanding of the properties of a variety of complex commercial alloys represents real progress in our overall knowledge of structure-property relationships.

### Acknowledgements

We are grateful to Gary Scarr for permission to use micrographs from his unpublished research in Figure 7. Preparation for this manuscript was supported in part by the Office of Naval Research.

### References

1. *'Titanium and Titanium Alloys'*, ASM Source Book (ASM, Metals Park, OH), 1982.
2. Chesnutt, J. C., Rhodes, C. G. & Williams, J. C., *ASTM STP 600*, (ASTM, Philadelphia, PA), 1976, p. 99.
3. Margolin, H., Chesnutt, J. C., Luetjering, G. & Williams, J. C., *'Titanium' 80, Science and Technology* (TMS-AIME, Warrendale, PA), Vol. 1, 1981, p. 169.
4. Hall, J. A., Pierce, C. M., Ruckle, D. L. & Sprague, R. A., *Mater. Sci. Engg.*, **9** (1972), 197.
5. Williams, J. C. & Starke, E. A., Jr., *'Deformation, Processing, and Structure'* (ASM, Metals Park, OH), 1984, p. 279.
6. Starke, E. A., Jr. & Luetjering, G., *'Fatigue and Microstructure'* (ASM, Metals Park, OH), 1979, p. 205.
7. Williams, J. C., *'Titanium Science and Technology'*, (Plenum Press, NY), Vol 3, 1973, p. 1433.
8. Blackburn, M. J. & Williams, J. C., *ASM Quart. Trans.*, **62** (1969), 398.
9. Welsch, G. & Bunk, W., *Metall Trans. A*, **13A** (1982), 889.
10. Williams, J. C. & Luetjering, G., *'Titanium '80 Science and Technology'* (TMS-AIME, Warrendale, PA), 1981, p. 671.
11. Luetjering, G. & Weissmann, S., *Acta Met.*, **18** (1970), 785.
12. Gysler, A., Luetjering, G. & Gerold, V., *Acta Met.* **22** (1974), 901.
13. Williams, J. C., Hickman, B. S. & Marcus, H. L., *Metall. Trans.*, **2** (1971), 1913.
14. Hombogen, E., *Z. Metallk.*, **58** (1967), 31.
15. Partridge, P. G., *Met. Rev.*, **12** (1967), 169.
16. Churchman, A. T., *Proc. Royal Soc.*, A. London, 226 (1954), 216.
17. Williams, J. C. & Blackburn, M. J., *Phys. Stat. Sol.*, **25** (1968), Ke.
18. Paton, N. E. & Williams, J. C. & Rauscher, G. P., *Titanium Science and Technology*, (Plenum Press, NY), Vol. 2, p. 1049.
19. Paton, N. E. & Backofen, W. A., *Metall. Trans.*, **1** (1970), 2839.
20. Williams, J. C., Sommer, A. W. & Tung, P. P., *Metall Trans.*, **3** (1973), 2979.
21. Cottrell, A. H., *'Dislocations and Plastic Flow in Crystals'*, (Oxford University Press), 1961, p. 4.24.
22. Paton, N. E. & Williams, J. C., *Proceeding of Second International Conference on Strength of Metals and Alloys*, (ASM, Metals Park, OH), vol. 1, 1970, p. 108.
23. Chakraborty, S. B., Mukhopadhyay, T. K. & Starke, E. A., Jr., *Acta Met.*, **26** (1978), 909.
24. Duerig, T. W., Terlinde, G. T. & Williams, J. C., *Metall Trans.*, **11A** (1980), 1987.
25. Swann, P.R., *'Electron Microscopy and the Strength of Crystals'* (John Wiley & Sons, New York), 1962, p.131.

26. De Fontaine, D., Paton, N. E. & Williams, J. C., *Acta Met.*, **19** (1971), 1153.
27. Froes, F. H., Yolton, C. F., Capenos, J. M., Wells, M. G. H. & Williams, J. C., *Metal Trans.*, **11A** (1980), 21.
28. Banerjee, D., Mukherjee, D., Saha, R. L. & Bose, K., *Metall Trans.*, **A**, **14A** (1983), 413.
29. Banerjee, D., Okada, M. & Williams, J. C., unpublished research, 1984.
30. Rhodes, C. G. & Paton, N. E., *Metall. Trans.*, **8A** (1977), 1749.
31. Hamajima, T., Luetjering, G. & Weissmann, S., *Metall Trans.*, **4** (1973), 847.
32. Crossley, F. A. & Carew, W. F., *Trans. AIME*, **209** (1957), 43.
33. Blackburn, M. J., *Trans. AIME*, **239** (1967), 1200.
34. Stroh, A. N., *Adv. Phys.*, **6** (1957), 418.
35. Petch, N. J., *J. Iron and Steel Inst.*, **174** (1953), 25.
36. Ritchie, R. O., Knott, J. F. & Rice, J. R., *J. Mech. Phys. Solids*, **21** (1973), 395.
37. Knott, J. F., *Fundamental of Fracture Mechanics* (Butterworths), 1979.